SPE 56823

Conditioning of Lévy-Stable Fractal Reservoir Models to Seismic Data

J. Gunning and L. Paterson, SPE, CSIRO Petroleum

This paper was prepared for presentation at the 1999 SPE Annual Technical Conference and Exhibition held in Houston, Texas, 3–6 October 1999.

Abstract

We have developed methods of conditioning non-stationary Levy-stable geostatistical models[1,2] to 3D seismic data. The technique involves adapting the sequential Levy simulation method such that the convolutional response of the realisations acceptably 'matches' the seismic amplitude map. A rejection scheme is used, which requires fast repetitive simulation of gridblock columns and generation of convolutional responses. The non–stationarity of the model means that this cannot be achieved using the conventional large kriging system. We use a different, but comparably rapid method, based on storing the relevant parts of a sequential simulation calculation for the column. Working directly with the amplitude traces also has the advantage of avoiding the ambiguities and non-uniqueness involved in inverting the traces to acoustic impedance.

The most difficult part of the problem is estimation of the seismic wavelet, and this is often done non-optimally. We describe a sophisticated method of estimating the wavelet, and show that this can yield better than expected results. Suitable rejection criteria are proposed, based on reasonable probabilistic models. The application of the technique is demonstrated with a field example.

Introduction

The use of geostatistical models to characterise uncertainty in the spatial distribution of petroleum reservoir properties is now seen as a fundamentally desirable tool in reserves or forecasting work. Production forecasts can follow a very wide distribution when reservoir heterogeneity is appreciable and where well data are sparse. For this reason, it is clear that the conditioning of these geostatistical models to auxiliary data like seismic and production data can only help in reducing forecasting uncertainties and thus the quality of management decisions.

Particularly in areas where well control of the underlying random field model is sparse, the sheer density of low-resolution measurements like seismic data will clearly constrain the range of variation seen in Monte-Carlo realisations of the random field. Nonetheless, it is currently impractical to condition the kinds of geostatistical models used in flow calculations to the full range of seismic data. Both for computational and storage reasons, the models are usually constrained only to post–stack, post–migrated data, which may represent only 5% or so of the total volume of data acquired.

In general, the relationship between remote–sensed acoustic properties of rocks with poor resolution (seismic data has resolution ≈ 30 m, at best) and local petrophysical properties with a small scale of support (≈ 1 m) is complex. Any credible conditioning method must take into account these very different scales of support. Most analysis rely implicitly on cross correlations modelled from the sonic and porosity logs, which implicitly assumes that the field scale seismic processing is consistent with the sonic log information.

The complexity of the relationship between seismic and petrophysical data also means that an analytical derivation of the posterior distribution of the petrophysical properties, conditional to the seismic data, is impossible in general. This conditioning must therefore be carried out using rejection–based sampling techniques like the Markov Chain Monte Carlo method: unconditional realisations are drawn, and rejected on the basis of their 'proximity' to the

observed data. In the case of seismic data, this proximity is usually determined by computing a 'synthetic seismic' from the unconditional reservoir realisation, and comparing this to the true seismic in some suitably meaningful way.

Such sampling techniques nearly always suffer from high rejection ratios when the conditioning is strong, so it is necessary that the algorithm used to draw realisations of the reservoir properties is extremely effecient. Furthermore, it is important that the *forward model* used to compute a 'synthetic seismic' from a given reservoir realisation must be simple and computationally rapid. Like other workers, we use a one–dimensional convolutional model, which expresses the amplitudes in a seismic trace at a given common midpoint as a convolution of the reflectivities in the geological profile immediately below.

To date, models along these lines have been successfully applied in the context of MultiGaussian models of the reservoir properties. A general theory for such models is given by Eide[3], in which the full posterior distribution for the reservoir properties is formally derived. In principle, this solution implies that posterior samples can be drawn explicitly, but the actual form turns out to be computationally infeasible. Some suggestions for suitable approximations to the posterior are given, in the context of a sequential simulation method, and some small-scale examples are given.

The work of Bortoli *et al*[4] uses the one-dimensional convolutional model also, but does not appeal to a full posterior distribution like that of Eide[3]. A rejection method is used, with the rejection criterion being a threshold correlation coefficient between the true and synthetic seismic which must be exceeded for the realisation to be accepted. For reasons to be explained later, we think this is not a particularly good choice of acceptance criterion, although it obviously guarantees a certain similarity between the true and synthetic seismic fields.

The methodology we present in this paper extends this previous work into a class of non–stationary, non–Gaussian random field models called Lévy fractal models. Techniques based on stationary models invariably require the removal of trend terms from the data, and this process can be very subjective. A less subjective technique would involve modelling the data with a general non-stationary processes, of sufficient 'elasticity' to accommodate the trends, but sufficiently parsimonious to enable adequate estimation of its parameters. Extensive analysis of the spatial behaviour of the *distribution* of increments in wireline log data[5−9] has shown that the distribution of increments usually has heavy tails and is well modelled by a Lévy–stable distribution. The heavy tails in the distribution yield a high probability of large 'jumps' in the spatial field, which aptly mimic the transitions across facies boundaries. Similarly, the width of this distribution as a function of the lag $\mathbf{r}$ used to form the increments frequently follows a power law behaviour, which betrays a quality of self-similarity akin to fractals.

Rapid sequential simulation techniques have been developed to generate hard–data conditioned realisations from these models, based on the idea of drawing samples from the conditional distribution of the increments about a given point, given fixed values at a set of neighbours[10]. But the analytical complexity of these models is such that developing a full posterior distribution for the reservoir properties additionally conditional to seismic data, along the lines of the theory given by Eide[3], is not possible or practical. Conditioning of these sequential methods to seismic data must therefore use a rejection method, as per Bortoli's work, but the rejection criterion will be established by drawing on insights from Eide's work.

The two main challenges in the problem are developing a statistically meaningful forward model to compute synthetic seismic data from realisations of the random field model, and secondly, deriving sensible acceptance criteria to ensure reasonable sampling of the posterior distribution.

The Levy Random Fractal model

The background and motivation of the development of Levy random field models is more amply presented in references[5,6,10]. The sequential algorithm used to draw realisations of the random field is very similar to that used in conventional sequential Gaussian simulation, with the following important exceptions. (1) The posterior distribution is developed for the *increment* between the grid-block to be simulated and a (presimulated of fixed) neighbour chosen as reference. (2) This posterior distribution is Levy–stable, with thick tails, not Gaussian. (3) The random path used in the sequential algorithm must visit the most isolated regions of space first, and gradually 'fill in the details' as the simulation proceeds. It has been shown that this choice of path is necessary to ensure the reproduction of the longest length scales of variability implicit in the fractal model.

For seismic conditioning, the sequential path has to be modified such that we simulate entire columns of grid-blocks at a time, until the column is 'accepted' and then proceed on to the next column. Commensurate with point (3) above, the path has been chosen to favour the most 'isolated' columns first, and then visit the nodes along each column in a sequence that visits the most isolated nodes first.

It turns out that the posterior distribution for a particular property at a generic node requires the Cholesky decomposition and subsequent inversion of a covariance–like matrix formed from the set of distances to the n nearest neighbours, typically about 20. The matrix does not depend on the values of these neighbours. Once this $O(n^3)$ calculation is performed, repeated samples can be drawn

in $O(n)$ flops *even if* the values of the neighbours change. Hence we can form an algorithm which computes repeat simulations of a large set of N nodes in $O(nN)$ flops, once the preliminary $O(Nn^3)$ work is performed for the first simulation. This depends on fixing the path through the set of N nodes, which in this case corresponds to the 'unknown' nodes of the selected column.

If the sequential path through the column of gridblocks is varied for each successive realisation, the $O(Nn^3)$ process of repeating these simulations is unacceptably slow. If we fix the path, the $O(nN)$ technique described in the preceding paragraph is applicable, and it works out that repeat simulations are at least 100 times faster than the first, which makes relatively high rejection ratios acceptable.

Apart from the context of seismic conditioning, it is clear that the technique just described will be useful in other conditioning problems, where certain subregions of the reservoir dominate the cost or rejection criteria proposed. A good example of this is the near–wellbore region in well–test conditioning problems.

Synthetic seismic and the wavelet

The one–dimensional convolutional theory used to model the relationship between acoustic rock properties at the short scale and seismic data starts with the relation

$$S(t) = w(t) * \frac{d\Phi}{dt}, \tag{1}$$

where $S(t)$ is the amplitude in the trace at time t, and $\Phi(t)$ is the acoustic impedance (density×velocity) at the depth z corresponding to t, in the vertical profile underneath the CMP corresponding to S. The wavelet $w(t)$ is a smoothing pulse that smears out the detail in $d\Phi(t)/dt$ to yield the amplitude $S(t)$. Because wireline log data is usually equispaced in depth z, and in cases where the relationship between t and z is approximately linear over the depth range of interest, we can rewrite the equation above in depth, with subtle but unimportant changes in the meaning of the notation:

$$S(z) = w(z) * \frac{d\Phi}{dz}. \tag{2}$$

The first problem is to estimate the wavelet w. We can generalise the problem by looking at Eq. (2) in Fourier space ($z \leftrightarrow k_z$). We have

$$S(k_z) = w(k_z) k_z \Phi(k_z) \tag{3}$$

and so the problem of estimating $w(k_z)$ can be seen as equivalent to the problem of estimating $w(k_z)k_z$, i.e. the derivative in Eq. (2) is immaterial to the problem (this is an important point, since we do not want to take numerical derivatives of noisy data). Likewise, the particular *property* represented by Φ is also not essential to the problem; if it is physically unrelated to S then this will show up in the 'regression statistics'. From these considerations, the problem can be seen to be a particular case of finding an optimal w to relate S and some property Φ via

$$S(z) = w(z) * \Phi(z). \tag{4}$$

There are other constraints on the problem. The wavelet w is likely to be *localised* in space (typically a few cycles at $\approx$ 30 Hz and $\approx$ 2.3 km/sec gives a few tens of metres), and will be bandlimited (say a few Hz to 100 Hz).

The localisation is probably the hardest constraint to impose, so we attack it directly by writing w as a set of convolutional coefficients a_k over some *finite* range $k = -N' \dots M'$ of the discretised data Φ. The convolved amplitudes $\mathcal{S}$ at the logging points $\mathcal{S}_j = \mathcal{S}(z_j)$ are then

$$\mathcal{S}_j = \sum_{k=-N'}^{k=M'} a_k \Phi_{j+k} + \bar{a}, \tag{5}$$

where we include the additional parameter $\bar{a}$ to soak up any zero-frequency offsets. To cast this as a regression problem, we minimise the squared difference between the 'true' seismic S, and the seismic $\mathcal{S}$ we would compute by using our derived $a_j, \bar{a}$ and the data Φ. We form an error χ^2 over all wells $i = 1 \dots N_w$ and over some subregion of the depths $j = j_{\min} \dots j_{\max}$ that interests us:

$$\chi^2 = \sum_{i=1}^{i=N_w} \sum_{j=j_{\min}}^{j_{\max}} \left(\sum_{k=-N'}^{k=M'} a_k \Phi_{i,j+k} + \bar{a} - S_{i,j} \right)^2. \tag{6}$$

The second index in $\Phi_{i,j+k}$ is allowed to wander outside $j = j_{\min} \dots j_{\max}$, providing there are data available, otherwise we pad with a suitable constant (usually $\langle \Phi \rangle$). **Fig. 1** gives a picture of the notation.

Since Eq. (6) is quadratic in the a's, its minimum is found in the usual way by differentiating with respect to the $a_k, \bar{a}$ and solving the resulting $N' + M' + 2$ size linear system. With N', M' of the order of a few hundred, this is not computationally difficult.

When the linear system is solved, it usually turns out the the wavelet w, represented as the discrete set of coefficients a_k, often looks quite 'noisy' (see **Fig. 2**). This noise represents high frequency content which cannot physically be present in the propagating sound wave, so we eliminate it by postprocessing the wavelet coefficients with a smoothing filter and fine tuning their weights. There are more rigorous ways of achieving this effect, involving the addition of bandwidth 'penalty' terms to Eq. (6), but these have not been implemented yet. After the smoothing has been performed, the resulting wavelet looks more physical (see **Fig. 2**).

Statistical significance of the optimal wavelet. The regression technique outlined in the previous section is of surprising power. This derives from the large amount of freedom in the large number $(N' + M' + 2)$ of parameters. It is important then not to be misled by the results of such a regression into believing that strong correlations exist between the seismic and well–log data. We sketch here a method of testing the significance of the regression, using a method akin to the probability calculation used with degree–of–correlation measures like the Kendall τ coefficient (see, e.g. section 14.6 of *Numerical Recipes*[11]).

For simplicity, imagine the case of one well and one seismic trace. We use these to generate an optimal wavelet and then compute some measure of association $r_{\rm true}$ (say the Pearson correlation coefficient[1]) between the real seismic trace and the 'synthetic trace' obtained by convolving the well data with the optimal wavelet. Now consider the null hypothesis that the well logs and the seismic are completely uncorrelated. We can make 'fake' well data that manifestly satisfy this condition by using the random field model and the simulation code to simulate well data using no hard or other constraints. These fake wells 'look' like the true well data, but are completely uncorrelated with it and the seismic trace. We then run the optimal wavelet calculation over an ensemble of such fake wells, and compute the same association measure $r^{(i)}_{\rm null}$ for each realisation i. The Monte–Carlo distribution of the deviates $\{r^{(i)}_{\rm null}\}$ can then be compared to the measured $r_{\rm true}$ to give an indication of how probable it is that the observed correlation is significant. For instance, if the $r_{\rm true}$ seems to lie in the upper 5% quantile of the Monte–Carlo $\{r^{(i)}_{\rm null}\}$ distribution, we might tentatively say we believe the correlation to be significant with one–sided probability 95%. The generalisation to the case of several wells is fairly obvious.

This method has been tested on the Stratton field data from the Bureau of Economic Geology[12], for which, unfortunately, no sonic logs are available. Nonetheless, a statistically significant (at the 5% level) wavelet can be developed using Φ as neutron porosity or the SP log.

'Cross-modelling' the true and synthetic seismic fields

Typically the wavelet $w(z)$ is obtained from a depth section significantly wider than the particular reservoir of interest. The regression routine will only perform sensibly if there are sufficiently many events in the seismic data, which means an interval of typically several hundred metres. The interval should not be too wide, so as to preserve an approximately linear relationship of time and depth.

A typical plot of the synthetic seismic $\mathbf{S}_{\rm synth} = \{\mathcal{S}_j\}$ and the true seismic $\mathbf{S}_{\rm true} = \{S_j\}$ at a well is shown in **Fig.3**. The column height of an actual reservoir to be simulated may be as little as a quarter wavelength on the scale shown. The problem is to find a meaningful way to relate these two signals over scales as relatively short as this. If, for example, we compute the Pearson cross-correlation coefficient ρ between the two traces, the statistic ρ varies significantly, depending on which interval we choose, and what well we examine. It is clear that ρ is likely to have a continuous, smooth distribution across the field, so imposing a acceptance threshold on ρ is not likely to sample from this distribution very well. Nor is it possible to develop this distribution from the raw well data alone; some extra modelling work is required.

It is clear that the two traces in this plot are spatially related, and exhibit very similar spatial characteristics. One can argue that the 'measured' seismic is likely to be the synthetic seismic, plus a data–and–measurement noise process filtered by the seismic processing and the earth's acoustic response to give an overall noise term of similar bandwidth to the actual signal. From this point of view, it is reasonable to model the two processes as a conventional joint multi-Gaussian process $\mathbf{S} = (\mathbf{S}_{\rm true}, \mathbf{S}_{\rm synth})$ with covariance

$$C_{\rm joint} = \begin{pmatrix} C_{11} & C_{12} \\ C_{12}^T & C_{22} \end{pmatrix}. \tag{7}$$

Furthermore, the similar spatial character of the true and synthetic fields indicates that the covariances C_{11}, C_{22}, C_{22} are likely to be very similar (the post–filtering operation in deriving the optimal wavelet can be adjusted to guarantee this). So as a working approximation (which can be generalised if required) we will model the joint covariance using

$$C_{\rm joint} = \begin{pmatrix} C & aC \\ aC & (a^2+b^2)C \end{pmatrix}, \tag{8}$$

where a and b are two constants introduced in this way to guarantee positive definiteness. The covariance C is modelled from the inverse Fourier transform of the spectral power density of the true and synthetic seismic traces, averaged over all wells. The constants a and b are estimated from simple one–point covariances.

The usefulness of the representation in Eq. (8) is that, if one were to generate realisations of the joint process using the usual Cholesky method[13], this would take the form

$$\mathbf{S}_{\rm true} = L.\mathbf{w}_1 \tag{9}$$

$$\mathbf{S}_{\rm synth} = a\mathbf{S}_{\rm true} + bL.\mathbf{w}_2. \tag{10}$$

Here the $\mathbf{w}_i$ are vectors of independent $N(0,1)$ deviates, and L is the Cholesky factor of C, $LL^T = C$. This last equation makes it clear that the ratio a/b is a measure of how 'similar' the processes are. If $a = 0$, they are independent; if $b = 0$, they are identical up to a scale factor. Numerical experiments have shown that, for data like

[1] any sensible measure can be used. The χ^2 error term of Eq. (6) is a good choice.

that illustrated in **Fig.3**, we nearly always have $a > b$ and $b \lesssim 0.5$. Furthermore, realisations of the joint process via Eq. (10) look very realistic compared to the seismic data along the wells as depicted in **Fig. 3**.

Having developed this model, the sampling problem amounts to the question: given the joint probability density function described above, what is the 'probability' of the realisation $\mathbf{S}_{\text{synth}}$, given $\mathbf{S}_{\text{true}}$? Just as there are no perfect tests of white noise, there is no ideal test for this question, but it is possible to form physically reasonable tests. The main point of a suitable test is to assess the cross–correlation.

From Eq. (10) it is clear that the quantity

$$\mathbf{S}_{\text{test}} = (\mathbf{S}_{\text{synth}} - a\mathbf{S}_{\text{true}})/b \tag{11}$$

has covariance C, so it is conceivable to test the power spectrum of this quantity against the power spectrum corresponding to C. This is a fairly tough test if b is small, as $\mathbf{S}_{\text{test}}$ will easily contain too much power unless $a\mathbf{S}_{\text{true}}$ is close to $\mathbf{S}_{\text{synth}}$. A simpler test, based on the same idea, is to compute the l_2 norm (sum of squares) of $\mathbf{S}_{\text{test}}$ and test this against the appropriate distribution. This is a weaker test, but eliminates the need for spectral density calculations during the simulation.

The comparison distribution for the l_2 norm is built by Monte-Carlo methods in a setup step. Using FFT methods, we generate many realisations of a process with covariance C, of length equal to the height of the column to be tested in the actual simulation. The l_2 statistic is formed for each of these, and an approximate distribution $p(l_2)$ is formed by binning the ensemble of l_2's, and normalizing such that the maximum of $p(l_2)$ is one. The distribution of $p(l_2)$ is, predictably, chi–squared like. The compactness of this distribution, and hence the rigour of the test, depend greatly on the height of the column to be simulated relative to the seismic resolution: a longer column means a tighter distribution $p(l_2)$ and hence a more exacting test. The overall work in this step is at most $O(10^7)$ flops, i.e. a few seconds on modern workstations.

During the simulation, the l_2 norm of the test vector $\mathbf{S}_{\text{test}}$ is computed, and a second, uniform deviate y is drawn. If $y < p(l_2)$ the realisation is accepted and we proceed to the next column; if not, another realisation of the column is drawn and the corresponding synthetic seismic formed, etc.

To illustrate the rigour of the test, consider the expectation of the l_2 norm of $\mathbf{S}_{\text{test}}$ when $\mathbf{S}_{\text{true}}$ and $\mathbf{S}_{\text{synth}}$ are drawn from the cross correlated model Eq. (10):

$$\langle l_2 \rangle_{\text{corr}} = \langle \mathbf{S}^2_{\text{test}} \rangle = \sum_i \lambda_i^2, \tag{12}$$

where the λ_i are the eigenvalues of C. If, however $\mathbf{S}_{\text{true}}$ and $\mathbf{S}_{\text{synth}}$ are drawn from a model with the *same* autocovariances but *zero* cross-covariance (i.e. the matrix in Eq. (8) with zero off–diagonal elements), the l_2 norm has expectation

$$\langle l_2 \rangle_{\text{uncorr}} = (1 + 2a^2/b^2) \sum_i \lambda_i^2. \tag{13}$$

Even for the relatively modest correlations $a = b = 0.5$, the ratio of these two expectations $\langle l_2 \rangle_{\text{uncorr}} / \langle l_2 \rangle_{\text{corr}} = 3$, so the test will reject a large proportion of the realisations from the wrong distribution. **Fig. 4** illustrates how very different the distribution of the l_2 norm is if the two signals are uncorrelated, compared to the correlated case.

An alternative test using l_2 norms can be derived from the question: for what linear combination $(\mathbf{S}_{\text{synth}} - a'\mathbf{S}_{\text{true}})$ is the ratio $\langle l_2 \rangle_{\text{uncorr}} / \langle l_2 \rangle_{\text{corr}}$, as computed using the assumptions above, a maximum? The answer is trivial to compute, and yields the coefficient $a' = \sqrt{a^2 + b^2}$, which is not too different from a when $a/b > 3/2$. For the example above, with $a = b = 0.5$, the norm ratio is ≈ 3.4.

Padding issues. One of the irksome aspects of this problem is that the spatial extent of the seismic wavelet is usually comparable to the height of the simulation region. This means that, in forming the synthetic seismic by convolution, padding effects pollute the synthetic seismic at the fringes of the simulation region, where the fringe width is equal to the appropriate offset N' or M' of the convolutional coefficients. Since there is little useful information in the polluted synthetic seismic data, the simulation region should be extended up and down by a number of gridblocks equal to the maximum of N', M'. The actual rejection algorithm will then operate only on the central, unpolluted synthetic seismic, and the 'fringes' of the simulation should be discarded.

Some Examples

We illustrate these ideas with two examples.

Synthetic Lévy motion example. We have constructed a large two dimensional example of fractional Levy motion, simulated on a 1024-node (depth)× 70-node (width) section. This 'truth case' fractional Levy motion field is filtered with a simple low order Ricker wavelet to produce a seismic field, as depicted in the top two images of **Fig. 5**. At the edges of the large field, wells are drilled, and the wavelet is estimated from seismic and log data along the wells, with extra noise introduced into the log data for realism. The recovered wavelet is shown inset on **Fig. 6**, where the true seismic signal and the synthetic signal obtained with the well logs and the estimated wavelet are shown on the left wiggle plots.

The spatial extent of the wavelet used was the range $-N' = -150$ to $M' = 150$ gridblocks, and the simple cross modelling technique described in the preceding section gave the coefficients $a = 0.78$, $b = 0.41$. To illustrate the validity of the 'intrinsic coregionalisation' hypothesis

in modelling the true and synthetic seismic covariances as $C_{11} = C_{22} = C_{12} = C$, we performed the following experiment. The power spectrum of $S_{\rm true}$, estimated using both wells and the full height of the original field (1024 points), was used, with the a, b as above, to produce a Monte Carlo ensemble of joint realisations. The auto and cross covariances were estimated for each of these realisations, and the ensemble of results used to compute standard errors for each of these covariances. The results are shown in **Fig. 7**. These indicate that the uncertainties are sufficiently great that the 'intrinsic coregionalisation' model cannot be rejected with any appreciable measure of uncertainty. In summary, because (i) the model is built typically using only a handful of wells, (ii) over a column height unlikely to be more than a few tens of seismic wavelengths, and (iii) because we force the seismic wavelet to give a very similar spectral density in the true and synthetic wavelets, it is very difficult to show that the intrinsic coregionalisation model is wrong.

Having estimated the wavelet, the seismic covariance C and the parameters a, b, the probability distribution of the l_2 norm of Eq.(11) is formed by a Monte Carlo simulation of seismic traces of length equal to the height of the column to be tested (150 blocks). Because the wavelet spreads information ± 150 blocks either side of this region, the region actually simulated is 450×70. **Fig. 8** shows 4 simulations conditioned to the wells, but not the seismic, and **Fig. 9** shows 4 realisations conditioned additionally to seismic data. Below each of the set of realisations in these figures is the corresponding synthetic seismic. The resemblance of the conditioned seismic images in **Fig. 9** to the 'truth case' of **Fig. 5** contrasts strongly to that of of **Fig. 8**, but the synthetic seismics are clearly not 'overconditioned'.

Stratton field example. The absence of sonic logs in this data set means that the correlations between seismic amplitudes and the non–sonic logs are bound to be weaker than could be obtained with sonic. Nevertheless, there is a statistically significant wavelet connecting porosity to amplitude (see **Fig. 2**). The intrinsic coregionalisation model gives coefficients $a = 0.62$, $b = 0.48$, which indicates a modest degree of independence, and a brief look at the well data convolutions of **Fig. 3** confirms this impression.

We aim to simulate porosity in the region of the C38 reservoir, at a depth of ≈ 1500 m. We construct a cross section which passes through the vertical wells 9 and 11, and use a fine grid of 0.3 m [1 ft] $\times$ 16.8 m [55 ft] $\times$ 16.8 m [55 ft] blocks, chosen to coincide with the seismic survey gridding, and the logging interval. Examination of the well logs shows that a simple, stationary exponential variogram model is applicable to this field, and such a simulation can be done as an 'special' case of the general Levy simulation algorithm, with stationary, exponential covariance. The major uncertainty here (as usual) is the horizontal range of the covariance. For porosity , we use the covariance structure $C(\mathbf{r}) = 0.0017e^{-3\sqrt{z^2+S_x^2x^2}/23.0}$ where all numerical coefficients except the anisotropy factor S_x have been obtained from the vertical variogram. With suitable stratigraphic adjustments, one can show that wells 9 and 11 correlate quite strongly, with an anisotropy factor of about $S_x = 0.004$.

We use this information in a 'suppressed data' estimation problem. The hard data in well 9 is suppressed, the anisotropy factor S_x is increased by a factor of three, and we simulate the data in well 9 using only hard data from well 11, but conditioned to the seismic. Three models were run, each of 200 realisations: (1) unconditioned to seismic, (2) conditioned to seismic using the covariance modelling described in the 'cross-modelling' section, (2) conditioned to seismic but accepting realisations whose $\chi^2 = |\mathbf{S}_{\rm synth} - \mathbf{S}_{\rm true})|^2$ is less than the value obtained at the calibration well (well 11). This last method is similar to the thresholding on the correlation coefficient used by Bortoli[4], and we include it for comparison purposes. **Fig. 10** illustrates the outcome of this numerical experiment.

The averages of the seismic–conditioned models are closer to the hidden data than the unconditioned model, as one would expect, but the effect of χ^2 thresholding is much stronger than the covariance criterion. The thresholding technique shows evidence of 'overconditioning': it improves the estimate in some regions and degrades it in others. The covariance technique affects the posterior distribution less strongly, but also with less bias.

The simulations show that the choice of acceptance criterion strongly influences the posterior distribution. The thresholding technique, because it never accepts half–reasonable candidates, tends to overcondition the posterior. The covariance modelling shows less dramatic effects, but is more justifiable from the original data and other physical grounds.

Future work

The last example highlights the importance of the sampling techniques used in these MonteCarlo rejection methods. There remains a significant problem in all of these 'column–based' modelling approaches, and that is that the choices made at each column are independent. In reality, the horizontal correlations in the fine scale model usually make adjacent columns look fairly similar. This means that a particular realisation of a column, if it is accepted with low probability, will tend to force subsequent simulations of nearby columns to be also relatively improbable. This effect ought to make the probability of acceptance of the original column lower, but because the algorithm proceeds on a column by column basis, these consequences cannot be incorporated into the algorithm as it stands. The overall effect is to make the synthetic seismic less

transversely continuous than the true seismic. It is possible to write down a theory which incorporates these ideas, but we leave the details of this to a later publication.

Conclusions

We have demonstrated that more complex, non-stationary random field models like the Lévy random fractal technique can be additionally conditioned to seismic data. The conditioning depends critically on having a fast repetitive simulation algorithm and a simple forward model to compute the 'synthetic seismic'. The amount of extra work required to condition simulations to seismic depends largely on the degree of correlation between synthetic seismics at well logs and the true seismic, and the number of gridblocks in the column to be simulated relative to the seismic resolution. Typically we suspect the extra time to be a factor between 2 and 10.

It is also possible to obtain statistically significant correlations with non–sonic logs, and perform simulations exploiting this correlation, but this will generally only be possible if the derived wavelet is optimised for this case. The extent to which a posteriori distribution is constrained by the seismic in this case depends strongly on the strength of the correlation obtained.

Furthermore, we have shown that the *a posteriori* random field distributions are relatively sensitive to the rejection criteria used in the sampling algorithm. We encourage other workers using similar algorithms to pay close attention to this matter, and hopefully stimulate further work in developing sound but computationally feasible algorithms.

Nomenclature

$S(t), S(z), \mathbf{S}_{\text{true}}$	seismic amplitude as a function of time t , depth z
w	seismic wavelet
$a_k, \bar{a}$	wavelet coefficients
Φ	well log property
k_z	Fourier wavenumber for depth
$\mathcal{S}, \mathbf{S}_{\text{synth}}$	Synthetic seismic
χ^2	mismatch error in optimisation
$C, C_{ij},\ i, j = 1, 2$	Covariance matrices between true and synthetic seismic
a, b	coefficients in covariance model
l_2	sum–of–squares norm of vector
λ_i	eigenvalues of C

References

1. Painter, S., Paterson, L. and Boult, P.: "Improved technique for stochastic interpolation of reservoir properties," *SPE Journal* (Mar. 1997) **2**, 48.

2. Gaynor, G.C., Chang, E.Y., Painter, S.L. and Paterson, L.: "Application of Lévy Random Fractal Simulation Techniques in Modelling Reservoir Mechanisms in the Kuparuk River Field, North Slope, Alaska," paper SPE 39739 presented at the 1998 SPE Asia Pacific Conference on Integrated Modelling for Asset Management, Kuala Lumpur, Mar. 23-24.

3. Eide, A.L.: "Stochastic Reservoir Characterization Conditioned on Seismic Data," *Geostatistics Wollongong '96*, Kluwer Academic (1997) .

4. Bortoli, L.J., Alabert, F., Haas, A. and Journal, A.: "Constraining Stochatic Images to Seismic Data," *Geostatistics Tróia '92*, Kluwer Academic (1993) .

5. Painter, S. and Paterson, L.: "Fractional Lévy Motion as a Model for Spatial Variability in Sedimentary Rock," *Geophysical Research Letters* (1994) **21**, 2857.

6. Painter, S.: "Evidence for Non-Gaussian Scaling Behavior in Heterogeneous Sedimentary Formations," *Water Resources Research* (1996) **32**, 1183.

7. Liu, K., Boult, P., Painter, S. and Paterson, L.: "Outcrop Analogue for Sandy Braided Stream Reservoirs, Permeability Patterns of the Triassic Hawkesbury Sandstone, Sydney Basin, Australia," *AAPG Bulletin* (1996) **80**, 1850.

8. Mehrabi, A.R., Rassamdana, H. and Sahimi, M.: "Characterization of Long-Range Correlations in Complex Distributions and Profiles," *Physical Review E* (1997) **56**, 712.

9. Liu, H.H. and Molz, F.J.: "Comment on "Evidence for Non-Gaussian Scaling Behavior in Heterogeneous Sedimentary Formations" by Scott Painter," *Water Resources Research* (1997) **33**, 907.

10. Painter, S.: "Numerical Method for Conditional Simulation of Levy Random Fields," *Mathematical Geology* (1998) **30**, 163.

11. Press, W.H. *et al.*: *Numerical Recipes The art of Scientific Computing*, second edition, Cambridge University Press (1992).

12. *3–D Seismic and Well Log Data Set. Fluvial Reservoir Systems–Stratton Field, South Texas*, Bureau of Economic Geology, The University of Texas at Austin.

13. Alabert, F.: "The practice of fast conditional simulations through the LU decomposition of the covariance matrix," *Mathematical Geology* (1987) **19**, 369.

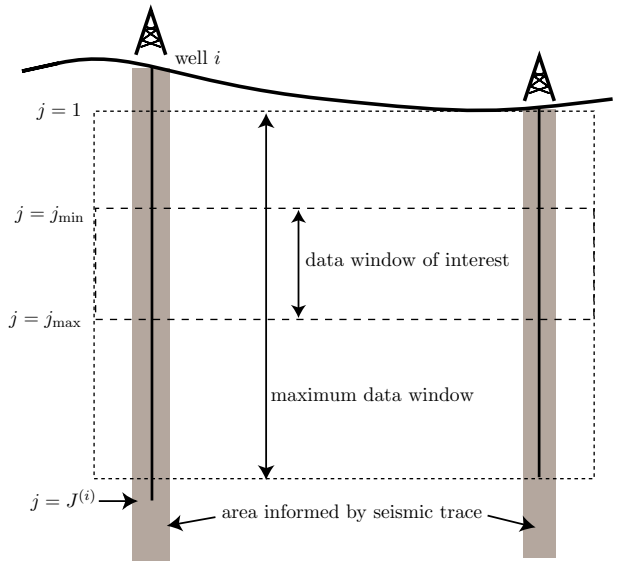

Fig. 1: Geometry and notation of technique for optimising the wavelet $w = \{a_i, \bar{a}\}$. There are N_w wells $i = 1 \ldots N_w$ with nearest seismic traces (depth–converted). We optimise the connection between the well property v and the seismic traces S over all wells and in the region of interest $j_{\min}, j_{\max}$.

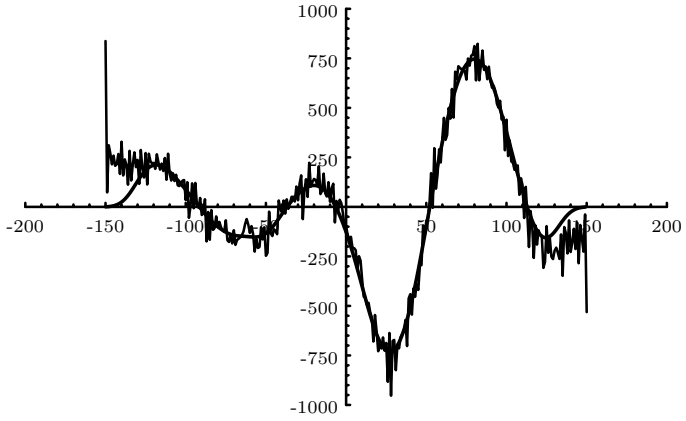

Fig. 2: Typical optimal wavelets produced by the regression routine for the Stratton Field data. The regression uses four wells and a 275 m [900 ft] interval logged at 0.3 m [1 ft] spacing to derive the wavelet. The noisy trace is the straightforward regression routine, the smooth curve shows the result with smoothing to constrain the bandwidth. Without smoothing, the Pearson linear correlation coefficients between the true (S) seismic and the computed convolutions $\mathcal{S}$ come out as $\{0.74, 0.84, 0.55, 0.57\}$, and after smoothing, we get $\{0.71, 0.83, 0.54, 0.57\}$. Adding extra constraints like bandwidth restrictions (i.e. smoothing) always degrades the correlation (in this case, not very much).

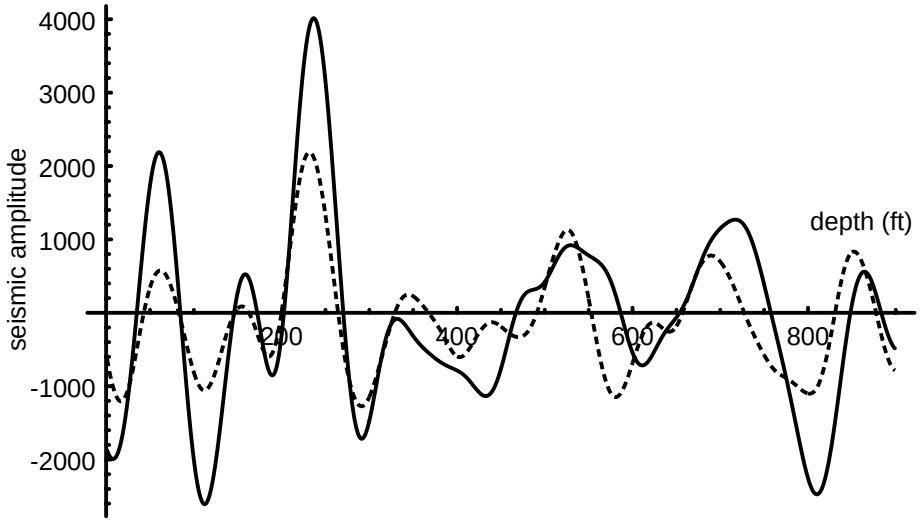

Fig. 3: Thick section of reservoir showing true seismic amplitude and 'synthetic amplitude' computed from a convolution of well–log porosity and an optimal wavelet. Conditioning directly to seismic traces requires estimating a realistic wavelet which will make these two traces closely resemble each other (the optimisation has been performed over a 275 m $[900$ ft] interval).

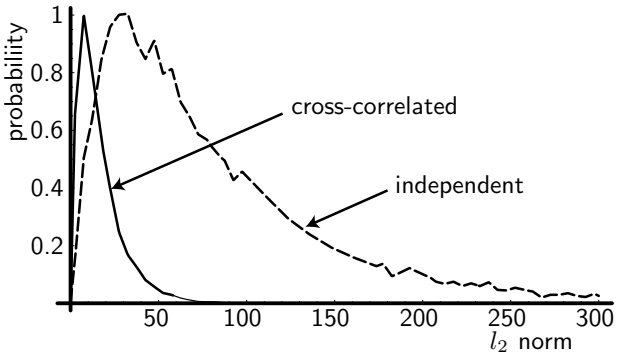

Fig. 4: The rejection distribution of the l_2 norm in the case of a correlated seismic/synthetic–seismic field with $a = 0.63$, $b = 0.48$, compared to the case if the two fields had the same self correlation but zero cross correlation. Probabilities developed by Monte Carlo, using a plausible Ricker power spectrum model for the covariance C, averaged on a column height of about $1\frac{1}{2}$ seismic wavelengths. Rejecting on the cross–correlated distribution of l_2 seems a reasonable idea.

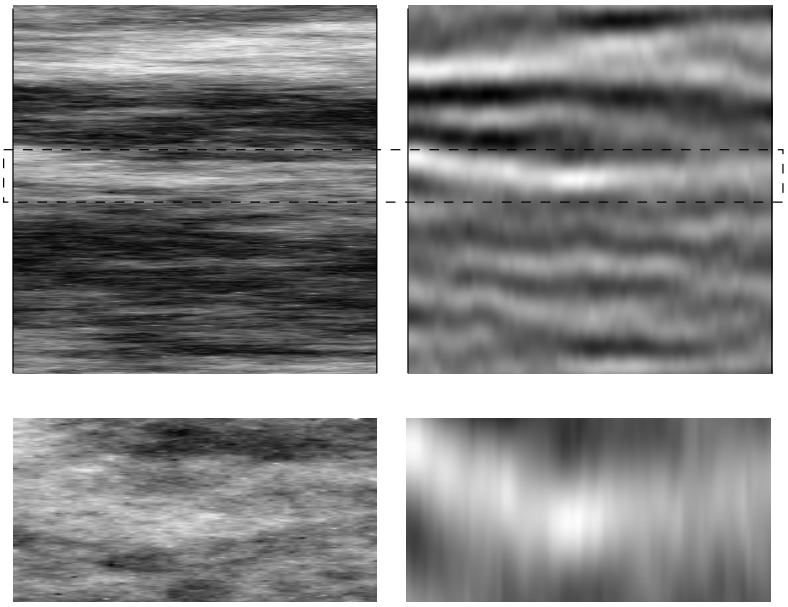

Fig. 5: Example showing large (1024×70) fractional Levy motion field with 2 wells 'drilled' at the edges, and an inner region for the actual study. The true field and the seismic in the region are shown expanded in the lower two figures.

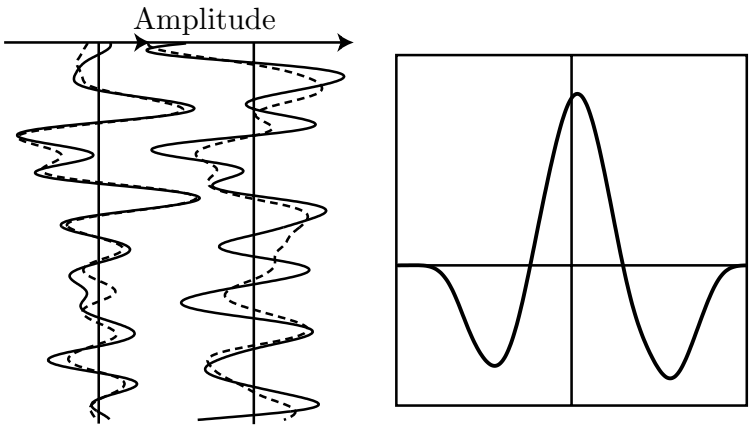

Fig. 6: True and synthetic seismic signals obtained at wells. drilled in edges of the large field of figure **5**. The synthetic trace is produced using the optimal recovered wavelet in the right–hand inset. The deviation from the perfectly symmetric Ricker form is due to the effect of noise.

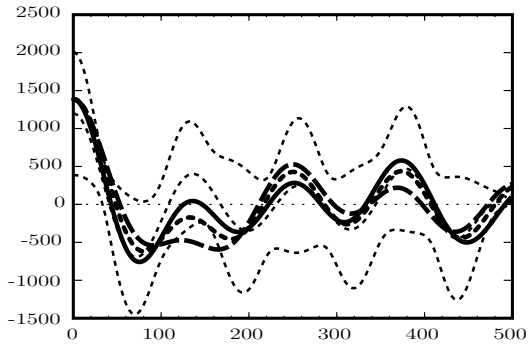

Fig. 7: Estimates of the auto and cross covariance function for the true and synthetic seismic signals. The thick solid line is the estimate of the true seismic covariance, from which a Monte–Carlo ensemble of joint realisations is made, using an FFT method. The mean and mean$\pm$one standard deviation curves of the covariance estimated from this ensemble are shown with the thinner dashed lines. The thick long–dashed line shows the sample synthetic seismic covariance from the well data, the thick short–dashed line the sample cross-covariance, normalised by $(a^2 + b^2)$ and b respectively. Both curves are well within reasonable error bounds associated with the intrinsic coregionalisation model, so may be satisfactorily modelled using the same covariance matrix.

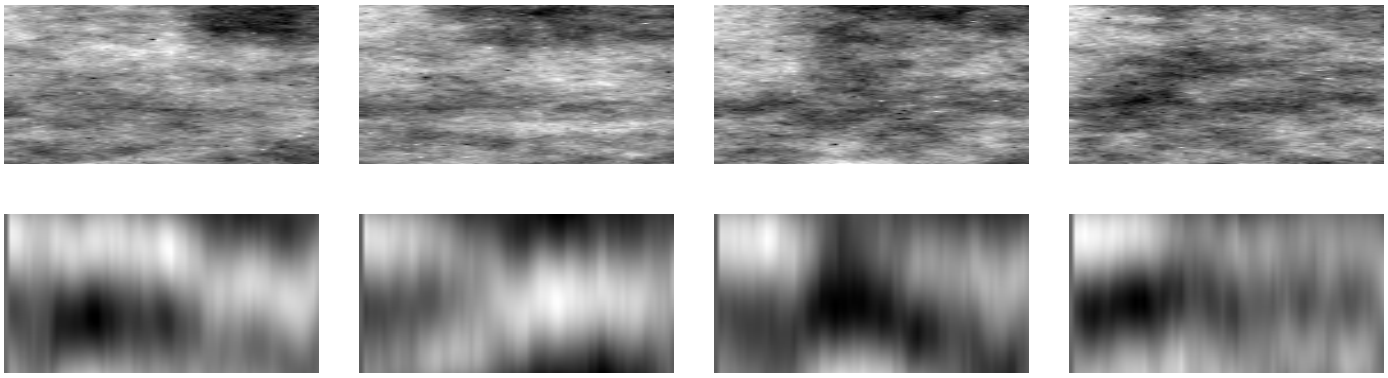

Fig. 8: Four realisations of the central region of **Fig. 5** conditioned only to the well data at the edges.

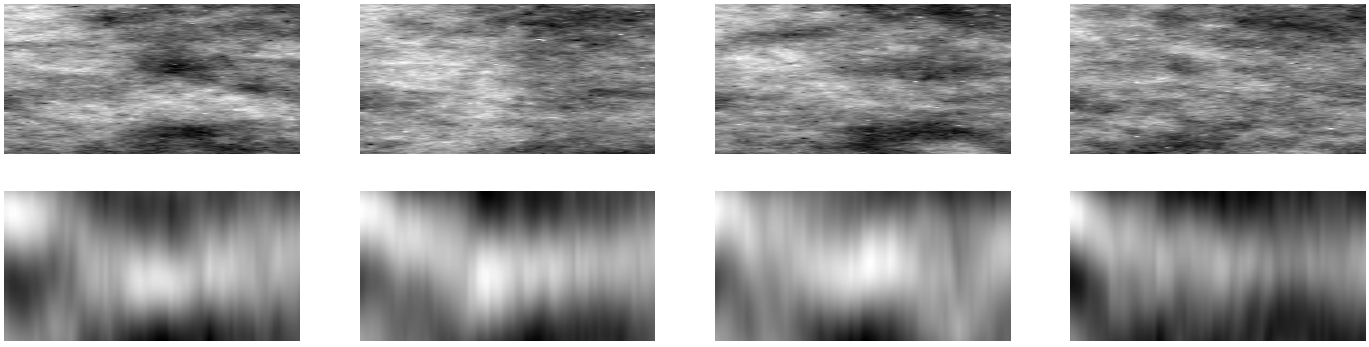

Fig. 9: Four realisations of the central region of **Fig. 5** conditioned both to the well data at the edges and the seismic.

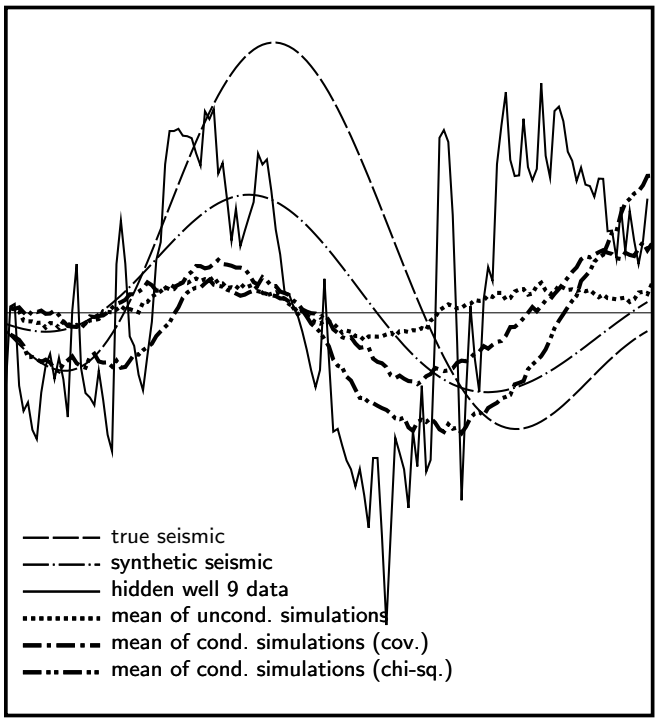

Fig. 10: Averages of simulating the hidden well data in well 9 based on well 11 data and seismic. Three methods were used. (1) Unconditional to seismic, (2) seismic with covariance modelling, (3) seismic with thresholding on $\chi^2 = |\mathbf{S}_{\text{synth}} - \mathbf{S}_{\text{true}})|^2$. The thick lines show *averages* of 200 realisations made using the three methods. Both seismic–conditioned methods do better than the unconditioned case, but the thresholding method is more dramatically affected. Thresholding on χ^2 is obviously a stronger constraint, but, as illustrated here, can improve estimates in some regions and degrade them in others.